7.1. Introduction

Zinc cobaltite ($ZnCo_2O_4$) is an attractive spinel structure in variety of applications that includes Lithium storage, photocatalytic activity, electrochemical sensing and also extending in the past 5 years to supercapacitors due to its low cost, high theoretical capacitance (2604 Fg^{-1}), facile preparation, excellent electrochemical stability and environment friendliness for supercapacitor applications. Several researchers have prepared the same compound with diversified preparation methodologies, say hydrothermal, combustion, electrodeposition, solvo-thermal methods. It is not well understood so far since each method with different researchers with different preparation conditions have yielded varied morphologies and results may it be photocatalysis or electrochemical. Under this situation, the works on $ZnCo_2O_4$ keeps on probed at and still more research is needed as the expected theoretical capacitance is yet to be reported. The different properties of $ZnCo_2O_4$ have been analysed by XRD, Raman, FESEM-EDAX, CV, GCD and EIS characterizations and the results are discussed in this Chapter.

7.2. X-Ray Diffraction Analysis of $ZnCo_2O_4$

The crystalline structure of the prepared Zinc cobaltite is validated by the XRD analysis and the obtained structure is refined with Rietveld refinement and shown in Figure 47. From the Rietveld analysis, the $ZnCo_2O_4$ sample demonstrates cubic spinel structure with $Fd\bar{3}m$ space group which is similar to the results published earlier **(Shanmugavalli et al., 2019).** The bottom blue line in the figure shows the difference in the experimental and the simulated diffractograms which is quiet flat indicating the best fit.

Table 17 provides the refined parameters obtained from the refinement such as W_R (weighed R factor), GOF (Goodness of fit) and other values. The obtained lattice parameter value from Rietveld analysis is 8.0859 Å with a good fit of W_R= 1.729 and GOF is 0.93. The lattice parameter value from JCPDS card No.: 23-1390 is 8.094 Å. This is very much close to the refined lattice parameter obtained. Hence it is concluded that the present sample falls in the spinel cubic structure. The Rietveld fit was done with polynomial background.

Using the Rietveld refined pattern of $ZnCo_2O_4$, atomic coordinates are identified using the VESTA software and is shown in Figure 48. In the unit cell of the refined crystal structure in Figure 48, oxygen atoms are located behind the Co atoms. Inset image represents the structure of the Zinc cobaltite without the cobalt atom to visualise the position of oxygen atom. In crystal structure, 'Zn' represents divalent cations in tetrahedral sites and 'Co' represents trivalent cations in octahedral sites of $ZnCo_2O_4$. In this structure, the oxygen anions form a cubic close-packed sub-lattice surrounded by tetrahedral and octahedral sites occupied by cations.

From Rietveld refinement of $ZnCo_2O_4$, the positional coordinates (x,y,z) of $ZnCo_2O_4$ are Zn at (0,0,0), Co at (0.625, 0.625, 0.625) and O at (0.3783, 0.3783, 0.3783) respectively. From the refined XRD analysis of $ZnCo_2O_4$, it is clear that the sample has sharp peaks without any secondary phase. It is a good sign regarding purity and high crystalline nature of the prepared sample. From Rietveld analysis, the number of atoms present are 21 Zn atoms, 8 Co atoms and 24 oxygen atoms are visualized using Vesta software. The (hkl) planes assigned by Rietveld refinement of $ZnCo_2O_4$ are noted corresponding to the respective XRD peaks of the prepared sample that matched with standard JCPDS card no 23-1390 **(Javed et al., 2019; Li et al., 2019)** and spinel cubic structure with $Fd\bar{3}m$ space group.

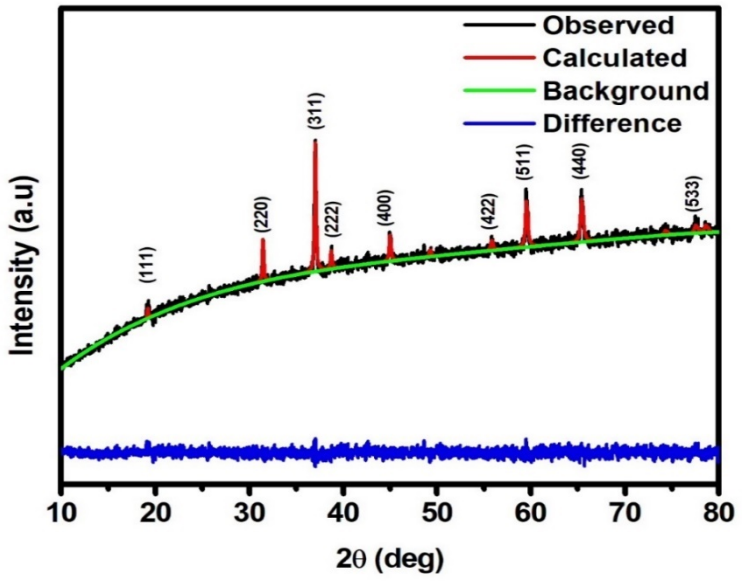

Figure 47 - Rietveld refined X-ray Diffractogram of $ZnCo_2O_4$

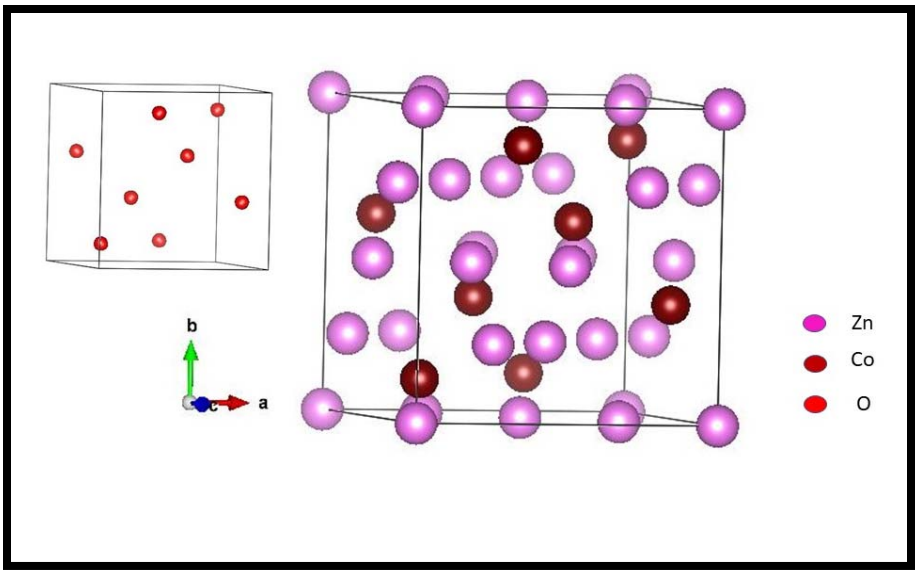

Figure 48 - Rietveld refined crystal structure of $ZnCo_2O_4$; inset shows the position of oxygen

The crystallite size calculated from the XRD analysis using Debye Scherrer formula is 30.45 nm. The parameters calculated from the XRD analysis are shown in Table 18.

Table 17 - Parameters obtained from the Rietveld refinements for $ZnCo_2O_4$

Sample/Parameter	**$ZnCo_2O_4$**
Crystal system /Space group	$Fd\bar{3}m$
Cell parameter (Å)	a=b=c=8.0859
Cell Volume ($Å^3$)	528.683
Co-Ordinates (x, y, z)	Zn (0.000, 0.000, 0.000) Co (0.625, 0.625, 0.625) O (0.387, 0.387, 0.387)
Occupancy	Zn: 1.059; Co: 1.058; O:1.086
Density (gm cm^{-3})	6.793
α, β, γ	90°
W_R	1.729
GOF	0.93

Table 18 - Parameters calculated from the X-ray diffractogram of $ZnCo_2O_4$

Sample / Parameter	2θ (311) (°)	β (311) (°)	d (311) (Å)	Crystallite size (nm)	Strain (ε)	Dislocation density ($x10^{15}$) /cm^3
$ZnCo_2O_4$	37.05	0.25	2.42	30.45	0.20	1.07

7.3. Raman Analysis of $ZnCo_2O_4$

Raman analysis is employed to further analyse the structural information of the prepared sample. For the analysis, He-Ne laser with a wavelength of 532 nm is employed as a source and the results of $ZnCo_2O_4$ is illustrated in Figure 49.

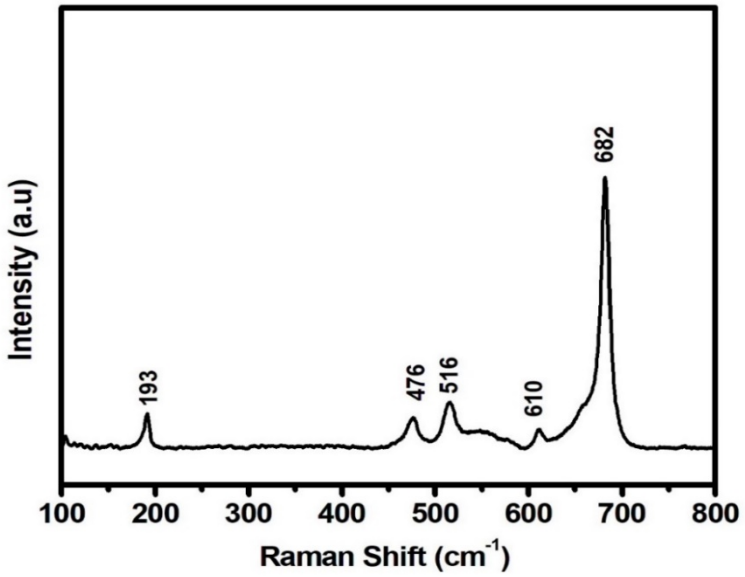

Figure 49 - Raman spectra of $ZnCo_2O_4$

Raman analysis of $ZnCo_2O_4$ shows five active modes ($E_g+A_{1g}+3F_{2g}$) in the region 100-800 cm^{-1}. The Raman peak at 610 cm^{-1} arises from the vibration of the Co-O bond which corresponds to the F_{2g} (1) symmetry mode. The band at 516 cm^{-1} is attributed to the F_{2g} (2) symmetry mode and the band at 476 cm^{-1} is due to the E_g symmetry species respectively. The peak at 193 cm^{-1} ascribes to the vibration of the Zn-O bond which is assigned to the F_{2g} (3) symmetry species. The high intense peak at 682 cm^{-1} originates from

the vibration of the Co-O bond which matches with the A_{1g} symmetrical mode. Similar observations are proposed by **(Ratha et al., 2015; Raut & Sankapal, 2017).** The Raman band assignments with relative vibrations for $ZnCo_2O_4$ is tabulated in Table 19. The modes of vibrations are illustrated in Figure 50 (**Foerster et al., 2012**).

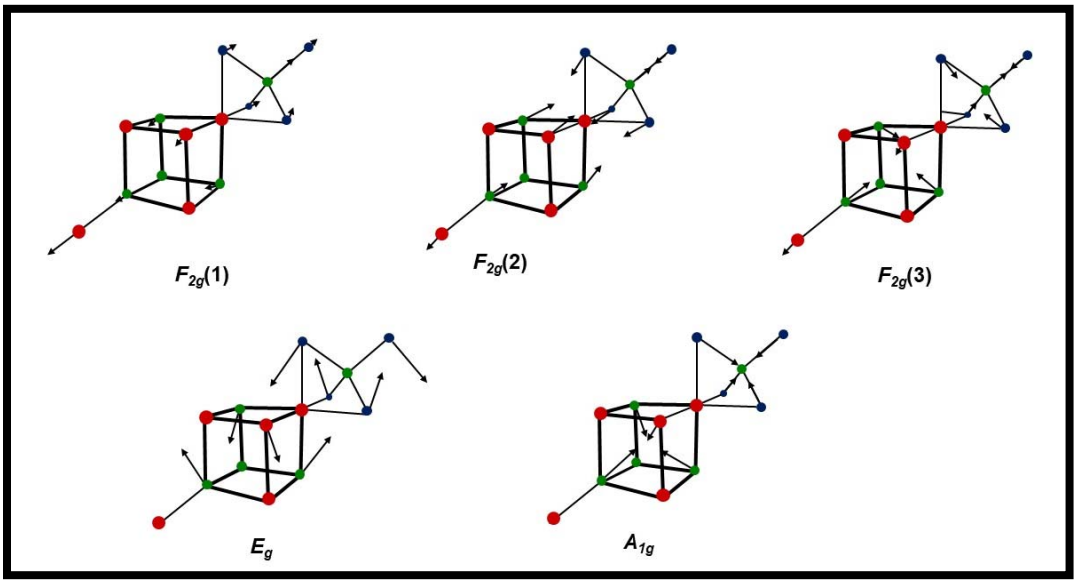

Figure 50 - Vibration modes of $ZnCo_2O_4$

Table 19 - Assignments of Raman peaks of $ZnCo_2O_4$

Raman Band (cm^{-1})	Symmetry species	Assignment
193	F_{2g} (3)	δ(Zn-O)
476	E_g	ν (Co-O) + ν (Zn-O)
516	F_{2g} (2)	ν(Co-O)
610	F_{2g} (1)	ν(Co-O)
682	A_{1g}	ν(Co-O)

7.4. FESEM Analysis of $ZnCo_2O_4$

Figure 51 illustrates the FESEM micrographs of $ZnCo_2O_4$. The magnification of x 98500 in 5µm scale shows the well-defined octahedral morphology with heterogeneous grain distribution. These micrographs exhibit the grain size of $ZnCo_2O_4$ exceeding 500 nm. Generally such discrete octahedral structures will be seen with hydrothermal process however the present work has achieved such discrete octahedral structure through optimized sol-gel process followed by calcination at 550°C for 5 hours (**Deng et al., 2018**).

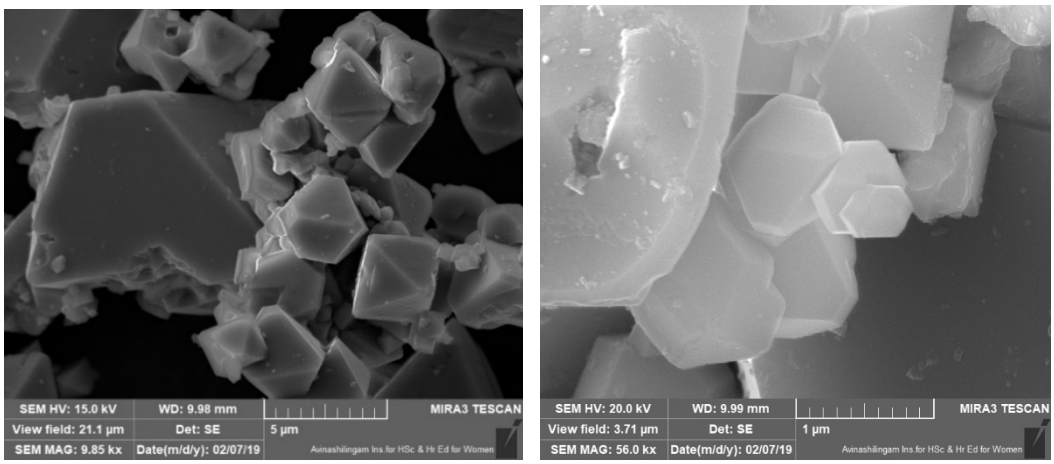

Figure 51 - FESEM micrographs of $ZnCo_2O_4$

7.5. Elemental Analysis of $ZnCo_2O_4$

Energy Dispersive X-ray Analysis (EDX) confirms the element present in the prepared sample. The EDX spectra are shown in Figure 52. In EDX spectra, the intense peaks at 0.772 eV and 0.525 eV corresponds to the Kα lines of Co and O respectively. The peaks at 1.013 eV and 6.923 eV are due to the presence of Lα lines of Zn and Co elements. In the prepared $ZnCo_2O_4$, no other peak than the expected is present which implies the purity of the sample. The atomic weight percentages of the elements are given in Table 20 and the obtained atomic weight percentages of Zn, Co and O elements are 6.32, 21.40 and 72.28 respectively.

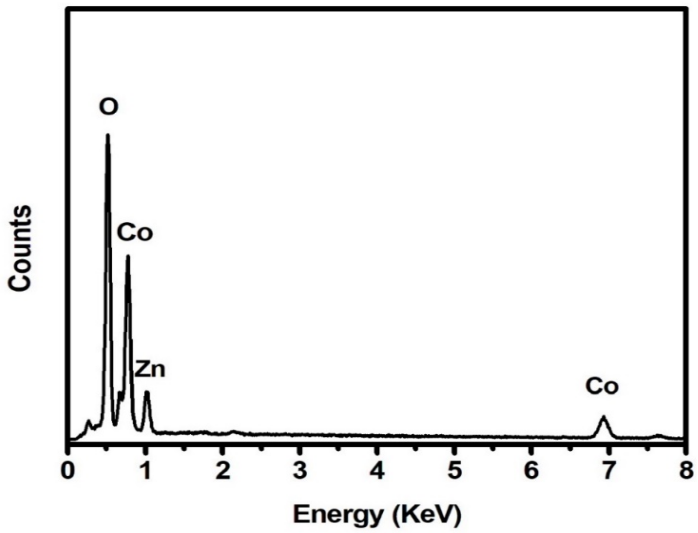

Figure 52 - EDX spectrum of $ZnCo_2O_4$

Table 20 - Elemental composition of $ZnCo_2O_4$

Elements	Atomic Weight %
Zn	**6.32**
Co	**21.40**
O	**72.28**

7.6. Electrochemical Analysis of $ZnCo_2O_4$

7.6.1. Cyclic Voltammetry Analysis of $ZnCo_2O_4$

Cyclic voltammetry analysis investigates the mass and electron transport properties of the prepared material. In this case, Zinc cobaltite has been examined and the results are discussed. The three electrode configuration of electrochemical cell consists of working electrode ($ZnCo_2O_4$), Ag/AgCl reference electrode and Pt counter electrode. Freshly prepared 1M KOH has been employed as the electrolyte for electrochemical analysis. With this standard three-electrode setup, the potential window of the working electrode in the CV analysis has been fixed from 0 V to 0.5 V after trials.

Figure 53 illustrates the CV analysis of $ZnCo_2O_4$ Vs Pt at various scan rates from 10 mV/s to 100mV/s. As can be seen, the shape of the CV indicates pseudo capacitive behaviour of Zinc cobaltite sample. Similar behaviour has been observed in previously reported results **(Vijaya kumar et al., 2017; Wang et al., 2014; Wu et al., 2015; Zhou et al., 2019)** The CV curve shows more or less a square curve between +0.2V to +0.45V. However, the stability of Pt has allowed the cyclability upto 0V. When increasing the scan rates, the peak current value also increases in the electrochemical system. This is due to the high electron drift in the electrode increasing the electrochemical kinetics at high scan rates. Hence, gradual improvement in the value of peak current with respect to scan rates is seen. However, there is no significant change in the shape of the CV curves even if the scan rate increases from 10 mV/s to 100 mV/s indicating the electrochemical stability of the system. The possible electrochemical reactions of $ZnCo_2O_4$ in alkaline medium as follows **(Song et al., 2017) .**

$$Co_2O_4^{2-} + H_2O + e^- \leftrightarrow 2\ CoOOH + 2OH^-$$

$$CoOOH + H_2O + e^- \leftrightarrow Co(OH)_2 + OH^-$$

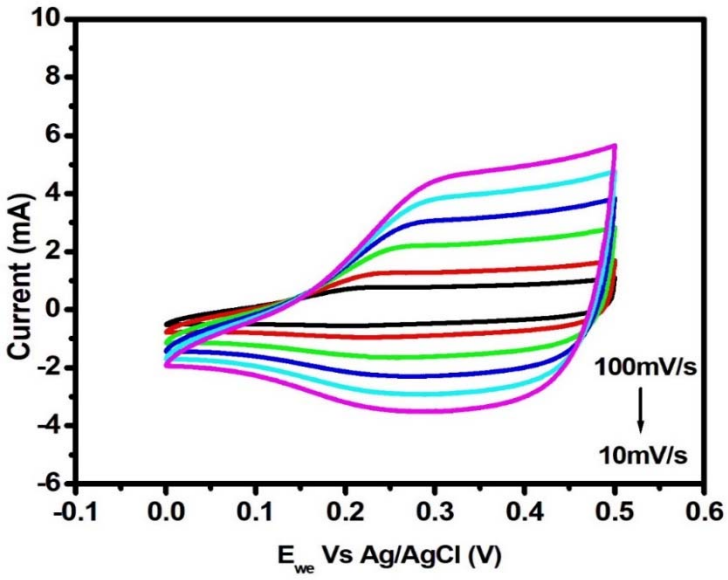

Figure 53 - Cyclic voltammogram of $ZnCo_2O_4$

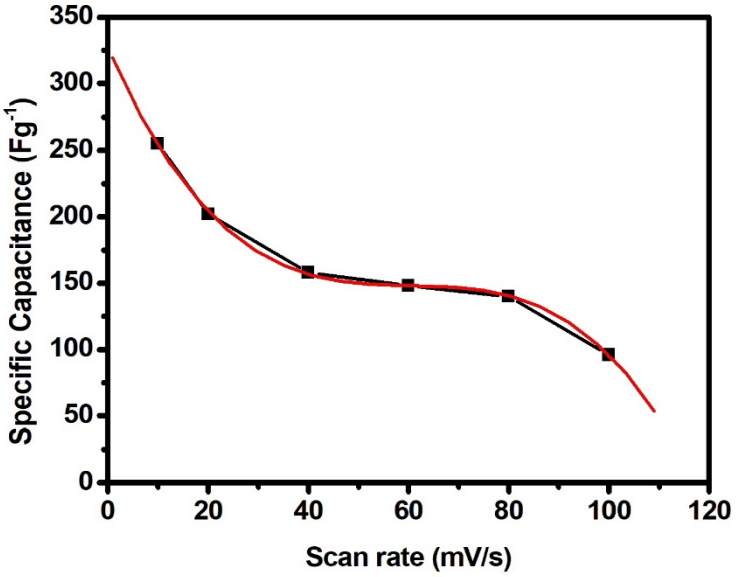

Figure 54 - Plot of scan rate vs specific capacitance of $ZnCo_2O_4$

The specific capacitances of the material from CV analysis are 255, 202, 158, 148, 140, 96 Fg^{-1} at the scan rate of 10 mV/s, 20 mV/s, 40 mV/s, 60 mV/s, 80 mV/s and 100 mV/s respectively. However, the specific capacitance decreases as the scan rate increases, falling from 255 Fg^{-1} at 10 mV/s to 96 Fg^{-1} at 100 mV/s, as shown in Figure 54. The following reasons may contribute to the reduction in specific capacitance with

scanning rate: (1) less contact between the surface of the electrode material with the KOH electrolyte at a high scan rate; (2) At a higher scan rate, the reaction of electrode material with electrolyte is inadequate. The polynomial fitted using Origin software showed third order dependency ($y=-7.89x10^{-4}x^3 + 0.1433x^2 -8.75221x +327.99$) indicating three different factors are involved such as ion accessibility, bulk conduction at the electrode and diffusivity in the interface. The scope of this work is not in identifying the exact reason and hence the investigation is not done here. However, a detailed investigation of thoughtful designing of experiment may offer better understanding on this aspect.

7.6.2. Galvanostatic Charge - Discharge Analysis of $ZnCo_2O_4$

Galvanostatic charge and discharge (GCD) analysis is performed to measure the voltage of the constructed electrochemical cell at a constant current and the corresponding GCD curve is shown in Figure 55. The shape of the GCD curve has deviated from a perfect triangular shape suggesting that the capacitance originates from pseudo capacitive mechanism and is consistent with CV results. In GCD analysis of Zinc cobaltite the charging time is shorter and the discharge time is longer thus offering more capacitance. The prepared Zinc cobaltite holds the maximum specific capacitance of 266 Fg^{-1} at a current density of 1 Ag^{-1}. Then, the specific capacitance value has decreased with increase of current density because insufficient active materials is involved in the faradaic reactions and the corresponding values are 213, 164, 145 and 132 Fg^{-1} at the current densities of 1.5, 2, 2.5 and 3 Ag^{-1} respectively. The obtained specific capacitance value is comparable with already reported literature. Table 21 gives the specific capacitance value of the previously reported literature of $ZnCo_2O_4$. From the Table 21, it is evident that most of the reported results exhibit higher specific capacitance than the present work. For example, **Reddy et al., (2020)** have prepared the $ZnCo_2O_4$ by hydrothermal method and attained 3D-hierarchical peony-like $ZnCo_2O_4$ structures with 2D-nanoflakes. The prepared $ZnCo_2O_4$ shows the specific capacitance of 421 Fg^{-1} when the prepared sample is coated on Ni foam **(Reddy et al., 2020)**. Samiei et al., 2021, have synthesized $ZnCo_2O_4$ nanoflowers by hydrothermal method. It exhibits a maximum specific capacitance of 572 Fg^{-1} using Ni foam as a current collector **(Samiei et al., 2021)**.

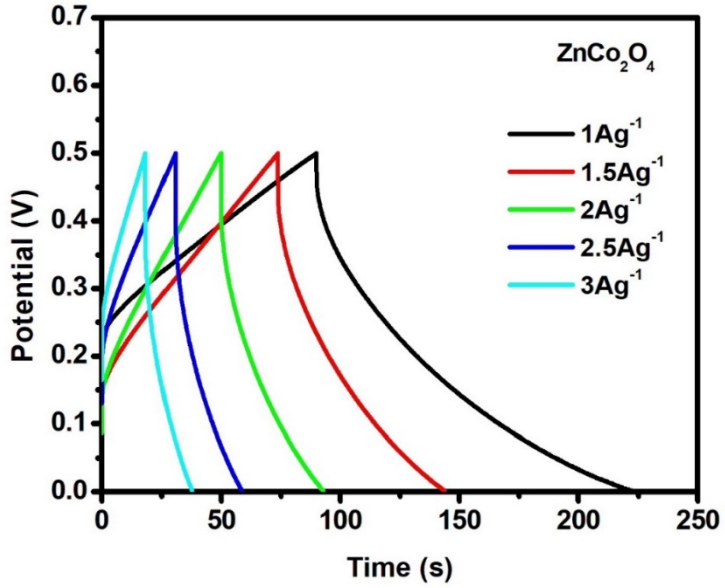

Figure 55 - Galvanostatic Charge-Discharge curves of $ZnCo_2O_4$

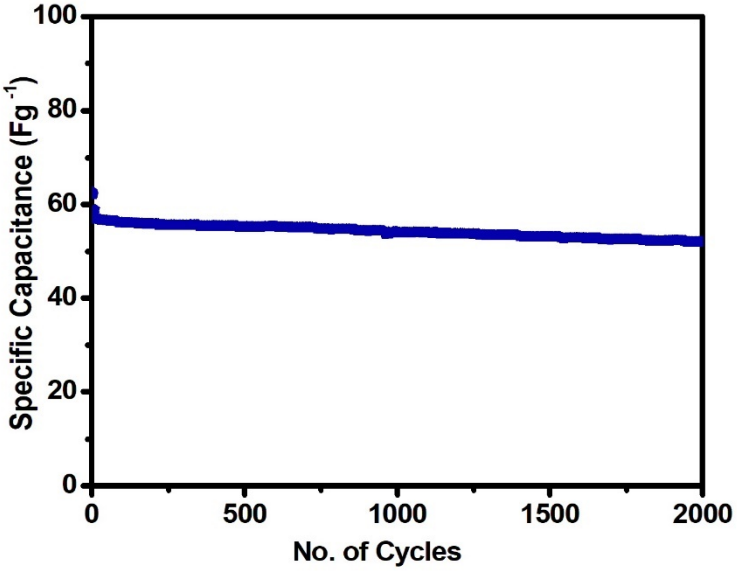

Figure 56 - Cyclic stability of $ZnCo_2O_4$

In the reported works, researchers have prepared the Zinc cobaltite by various techniques other than the sol-gel method. Also, they have attained better electrochemical performance when using Ni foam as the current collector. But cost of the Ni foam and the preparation of Ni foam is high. Hence, the cost of the device goes high while using Ni foam current collector. In the present work, $ZnCo_2O_4$ have been prepared by sol-gel method and the working electrode is coated on cost-effective copper foil.

The electrochemical stability of the prepared $ZnCo_2O_4$ sample coated on copper foil is tested at a current density of 5 Ag^{-1} over 2000 cycles by charge-discharge analysis, shown in Figure 56. After 2000 continuous charge-discharge cycles, 82.2% of specific capacitance has been retained suggesting that the sample has better cyclic stability.

Table 21 - Comparison of specific capacitance of $ZnCo_2O_4$ value with various literature

Material	Preparation method	Current collector	Specific capacitance (Fg^{-1})	References
$ZnCo_2O_4$ nanoflowers	Hydrothermal	Ni foam	472 @ 0.5 Ag^{-1}	**Samiei et al., 2021**
$ZnCo_2O_4$	Reflux condensation approach	flexible stainless-steel mesh	315 @ 2mA/cm^2	**Kamble et al., 2021**
$ZnCo_2O_4$	Co-precipitation	Ni foam	159 @ 2mA/cm^2	**Silambarasan et al., 2021**
$ZnCo_2O_4$ Nanospinels	Condensation	Graphite sheet	177 @ 0.25 Ag^{-1}	**Parveen et al., 2020**
$ZnCo_2O_4$	Hydrothermal	Ni foam	61 @ 0.5 Ag^{-1}	**Yang et al., 2020**
peony-like $ZnCo_2O_4$	Hydrothermal	Ni foam	421@ 1 Ag^{-1}	**Reddy et al., 2020**
$ZnCo_2O_4$ nanoparticles	Hydrothermal	Ni foam	434 @ 5 mV/s	**Priya et al., 2019**
Microspheres $ZnCo_2O_4$	Hydrothermal	Ni foam	689 @ 1 Ag^{-1}	**Chen et al., 2019**
$ZnCo_2O_4$ hexagonal nanoplates	Co-precipitation	Ni foam	133 @ 1 Ag^{-1}	**Bhagwan et al., 2019**
$ZnCo_2O_4$ microspheres	Hydrothermal	Ni foam	500 @ 0.75 Ag^{-1}	**Saravanakumar et al., 2019**
$ZnCo_2O_4$ nanomaterial	Hydrothermal	Ni foam	290 @ 0.5 Ag^{-1}	**Mary & Bose, 2018**
hollow $ZnCo_2O_4$ microspheres	Solvothermal	Ni foam	284 @ 1 Ag^{-1}	**Shang et al., 2018**
peony-like $ZnCo_2O_4$	Solvothermal	Ni foam	440 @ 1 Ag^{-1}	**Shang et al., 2017**
Coral -like $ZnCo_2O_4$ nanowires	Hydrothermal	Ni foam	694 @ 2 Ag^{-1}	**Rajesh et al., 2017**
$ZnCo_2O_4$ Microspheres	Solvothermal	Ni foam	542 @ 1 Ag^{-1}	**Gai et al., 2017**
$ZnCo_2O_4$ Microspheres	Solvothermal	Ni foam	689 @ 1 Ag^{-1}	**Fu et al., 2015**
$ZnCo_2O_4$	**Sol-gel method**	**Cu foil**	**266** @ 1 Ag^{-1}	**This work**

7.6.3. Electrochemical Impedance Analysis of $ZnCo_2O_4$

Electrochemical impedance analysis (EIS) has been performed in the frequency range between 100 mHz to 10 KHz with 1M KOH electrolyte solution in three-electrode configuration. In Nyquist plot, high frequency and intermediate frequency region involves solution resistance and charge transfer resistance which are obtained from the intercept at the Re(Z) and diameter of the semicircle as shown in Figure 57. It shows that the prepared $ZnCo_2O_4$ sample exhibit an incomplete semi-circle followed by a spike in the low frequency region which associates with diffusion process and solid electrode and electrolyte interfacial reaction.

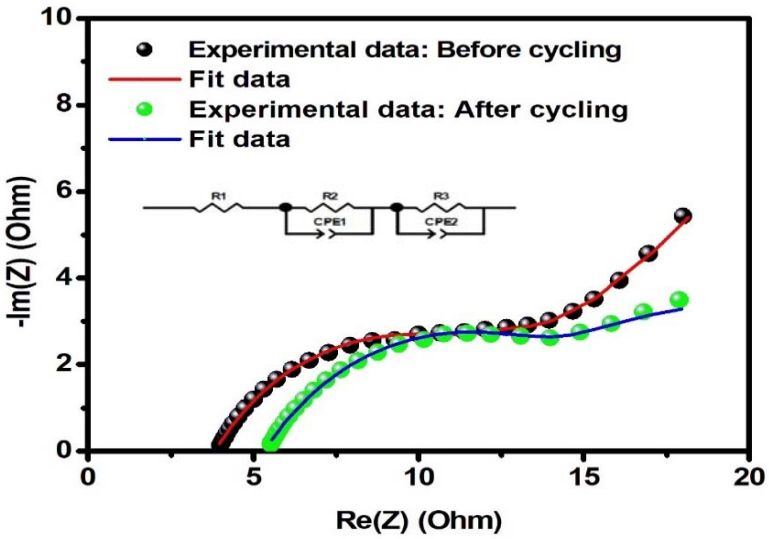

Figure 57 - Electrochemical impedance spectra of $ZnCo_2O_4$

The observed Nyquist plot is fitted with theoretical simulation, and the corresponding equivalent circuit is shown in the inset. The fitted parameters are listed in the Table 22. The fitted equivalent circuit contains two tank circuits with resistance parallel to the constant phase elements. Before cycling, the value of solution resistance (R_1) and the charge transfer resistance (R_2) for $ZnCo_2O_4$ are 3.81 Ω and 3.92 Ω respectively. After 2000 numbers of cycling, there is a mild increment in the solution resistance indicating stability of the electrolyte on cycling, but the charge transfer resistance became 26.6 Ω which means there is a barrier created due to cycling in the interface contributing

to the internal resistance of the cell. Looking into the capacitive behaviour through the CPE element, one order decrement in capacitive value shows that there is diffusion mechanism occurring in the electrochemical system and the extent of which is estimated with the n1 values before and after which has gone from 0.59 to 0.63.

Table 22 - Fitted parameters of electrochemical impedance spectra of $ZnCo_2O_4$

Parameters	$ZnCo_2O_4$	
	Before Cycling	**After Cycling**
$R_1(\Omega)$	3.81	5.31
$R_2(\Omega)$	3.92	26.6
CPE 1	0.07	7.56×10^{-3}
n1	0.59	0.63
$R_3(\Omega)$	11.33	191
CPE 2	0.14	6.17×10^{-3}
n2	0.63	0.47

As n1 is the measure of dispersion in the electrochemical impedance analysis, the increase in value conveys that the capacitive behaviour is preserved in the aspect of charge transfer on the electrode. The third component of the circuit R_3 and CPE2 clarifies on the diffusion aspect of the interface and hence the capacitance has gone too low with two orders magnitude indicating the severe diffusion behaviour of the interface The resistance has gone from 11 Ω to 191 Ω indicating the explaining of diffusive resistance increment with the dispersion being reduced in the aspect of resistive behaviour of the interface. Thus, the standard electrochemical system constructed with pure $ZnCo_2O_4$ as working electrode demonstrates the behaviour of the working electrode as capacitive but have severe diffusive effect on the interface.

7.7. Summary

From structural characterizations (XRD and Raman analysis) it is confirmed that the $ZnCo_2O_4$ exhibits cubic spinel structure with $Fd\bar{3}m$ space group. The sharp and intense peaks in XRD analysis exhibit a high crystalline nature of the sample. The FESEM images show octahedral morphology with the grain size in the range of 400 nm. EDX analysis

shows the presence of Zn, Co and O elements without any impurities validating the purity of the sample. The electrochemical properties of Zinc cobaltite exhibit pseudo capacitive behaviour with a maximum specific capacitance of 266 Fg^{-1} at current density of 1 Ag^{-1}. Before cycling, the charge transfer resistance of the sample from the electrochemical impedance analysis is 3.92 Ω and 82.2% of initial specific capacitance has been retained even after 2000 cycles revealing the cyclic stability of the sample. In summary, the better performance has been attained in Zinc cobaltite by simple sol-gel method demonstrating suitable electrode material for supercapacitor applications.